Single-Molecule Force Imaging Reveals That Podosome Formation Requires No Extracellular Integrin-Ligand Tensions or Interactions

Kaushik Pal[1], Ying Tu[1], Xuefeng Wang[1,2]*

[1]Department of Physics and Astronomy, Iowa State University, Ames, IA 50011, USA

[2]Molecular, Cellular, and Developmental Biology interdepartmental program, Ames, IA 50011, USA

[*]To whom correspondence may be addressed. Email: xuefeng@iastate.edu

ABSTRACT: Podosomes are integrin-mediated cell adhesion units involved in many cellular and physiological processes. Integrins likely transmit tensions critical for podosome functions but such force remains poorly characterized. DNA-based tension sensors are powerful in visualizing integrin tensions but subject to degradation by podosomes which ubiquitously recruit DNase. Here, using a DNase-resistant tension sensor based on a DNA/PNA (peptide nucleic acid) duplex, we imaged podosomal integrin tensions (PIT) in the adhesion rings of podosomes on solid substrates with single molecular tension sensitivity. PIT was shown to be generated by both actomyosin contractility and actin polymerization in podosomes. Importantly, by monitoring PIT and podosome structure in parallel, we showed that extracellular integrin-ligand tensions, despite being critical for the formation of focal adhesions, are dispensable for podosome formation, as PIT reduction or elimination has an insignificant impact on structure formation and FAK (focal adhesion kinase) phosphorylation in podosomes. We further verified that even integrin-ligand interaction is dispensable for podosome formation, as macrophages form podosomes normally on passivated surfaces that block integrin-ligand interaction but support macrophage adhesion through electrostatic adsorption or Fc receptor-immunoglobin G interaction.

KEYWORDS: single-molecule force, tension sensor, podosome formation, podosome force, integrin tension, macrophage

Podosomes are adhesive membrane structures commonly found in macrophages, dendritic cells, osteoclasts, and other cell types.[1-3] Interacting with the extracellular matrix (ECM) both mechanically and biochemically,[4-7] podosomes play a crucial role in cell motility, immune surveillance, bone structure maintenance, development and organogenesis.[8-10] With a diameter of 0.5-2 μm, a typical podosome consists of a dense F-actin core and a surrounding adhesion ring,[1, 4] which are connected by peripheral actin network loaded with myosin II.[11] The core region recruits both proteases and DNase that degrade matrix protein and extracellular DNA,[12] whereas the adhesion ring recruits integrins that mediate cell-matrix adhesion.[13] As transmembrane proteins, integrins bind to ligands on the matrix by the extracellular domains. The intracellular domains of integrins are hinged to cytoskeleton through an array of adaptor proteins such as talin, vinculin, paxillin, FAK (focal adhesion kinase), *etc.,* hence establishing a linkage between cells and the matrix. Integrins and these associated proteins are also recruited to focal adhesions (FA), another major type of cell adhesive units. It has been well known that integrins in FAs transmit force which participates in mechanotransduction and critically mediates FA formation and maturation.[14-17] It seems within plausible extrapolation to assume that integrins in podosomes also transmit tensions which might serve as important biomechanical cues for podosome formation. However, compared to the well-studied integrin tensions in FAs, integrin tensions in podosomes (podosomal integrin tension, or PIT) have been less characterized, and the role of integrin tensions in podosome formation is uncertain. The scarcity of PIT study is mainly due to the small size of podosomes and the likely weak adhesive force that demands high resolution and sensitivity from cell adhesive force imaging techniques.

In recent years, DNA-based fluorescent tension sensors have demonstrated piconewton (pN) sensitivity and submicron resolution in visualizing integrin tensions in FAs.[18-22] However, podosomes ubiquitously recruit membrane-bound DNase that readily degrades DNA-based sensors, [12] compromising their applications in PIT imaging. Lately, Glazier R. *et al.* applied DNA hairpin-based tension probes to visualizing integrin tensions in podosome-like structures formed in fibroblasts elicited on fluidic lipid substrate.[23] These podosome-like structures may not recruit DNase, hence being amenable to DNA-based tension sensors. However, fibroblasts do not naturally form podosomes, and the podosome-like structures on the fluidic lipid substrates likely have biomechanical behavior deviating from podosomes formed on solid substrates. Overall, PIT

in podosomes on solid substrates have not been visualized and studied. The relation between PIT and podosome formation remains unexplored.

Previously, to visualize adhesive force of DNase-rich cells such as cancer cells,[24] we developed peptide nucleic acid (PNA)/DNA hybrid-based integrative tension sensor (ITS) that tolerates DNase.[25] This DNase-resistant ITS has been shown to efficiently report cell adhesive force in DNase-present environment, therefore offering a feasible approach to study integrin tensions in DNase-laden podosomes. With the DNase-resistant ITS, we visualized PIT with single molecular tension sensitivity, confirming that integrins transmit force in the adhesion rings of podosomes. We further monitored the temporal and spatial dynamics of PIT, and revealed its force sources. Surprisingly, by co-imaging force and structural proteins in both podosomes and FAs, we revealed that podosome formation, in contrast to FA formation, is independent of PIT transmitted by integrin-ligand bonds.

RESULTS AND DISCUSSION

DNase-resistant tension sensor reports integrin tensions in podosomes on solid substrates

DNA-based tension sensors have become powerful techniques for imaging cell adhesive forces at cell-substrate interfaces, owing to the programmable tension detection ranges and convenient synthesis. Fluorescent tension sensors based on dsDNA or DNA hairpin have been developed and successfully applied to reporting integrin tensions in many types of cells such as keratocytes, platelets, T cells, *etc.*[21, 26, 27] Lately, we found that both podosomes and invadopodia consistently recruited membrane-bound DNase X (Figure 1A), which readily degrades DNA-based sensors.[12] Our early attempts of using DNA-based tension sensors to study podosomal adhesive force indeed suffered from sensor degradation and false signal caused by DNase in podosomes (Figure S1A and 1B). Therefore, the strong DNase activity in podosomes compromises the application of DNA-based tension sensors in podosomal force study.

To overcome this issue, we developed DNase-resistant integrative tension sensor (ITS) using a PNA/DNA hybrid duplex as the force-sensing construct.[25] An 18 base-paired PNA/DNA duplex is conjugated with a cyclic peptide RGD (Arg-Gly-Asp) as the integrin ligand,[28] a quencher-dye pair and a biotin as shown in Figure 1B. This PNA/DNA construct exhibits strong resistance to

DNase in podosomes as shown in Figure S1C. The DNase-resistant ITS is immobilized on a glass surface through biotin-neutravidin interaction where the peptide ligand of ITS is accessible to integrins in podosomes. Fibronectin is also doped in the surface coating to support cell adhesion and minimize the potential impact of ITS rupture to cell functions. Integrin molecular tension greater than the tension tolerance (T_{tol}, 12 pN for unzipping a PNA/DNA duplex) of ITS has a high probability to dissociate the duplex,[18] hence freeing the fluorophore from quenching and activating the ITS to fluoresce (Figure 1B). This process converts invisible force into fluorescence and enables integrin tension imaging. We tested DNase-resistant ITS in imaging podosomal integrin tension (PIT) in THP-1 cells, which form abundant podosomes after being transformed into macrophage-like cells using tumor growth factor-β1.[29] On the ITS-immobilized surface, we successfully observed ring-patterned force signal colocalized with the adhesion rings marked by immunostained vinculin (Figure 1C and Figure S1D), verifying the feasibility of ITS in the study of PIT. A control test in Figure S1E showed that PNA/DNA-based ITS without RGD exhibited no fluorescent signal at podosome sites, confirming that PNA/DNA-based ITS indeed resists podosomal DNase and reports integrin tensions specifically. Intensity analysis over the fluorescence signal in single podosomes shows that the adhesive force is in a ring or a donut pattern (Figure 1D).

Temporal dynamics of PIT

Podosome structure is known to be highly dynamic.[30, 31] Using DNase-resistant ITS, we studied the temporal dynamics of podosome adhesive force by imaging PIT. THP-1 cells were plated on ITS-immobilized surface and time-lapse imaging was performed on the live cells with a TIRF (total internal reflection fluorescence) microscope. Two force imaging modes have been adopted in the PIT imaging. Because ITS activation by force is irreversible, PIT imaging at a single time point is naturally in cumulative mode which collects all PIT signals generated in the past. This imaging mode greatly enhances force signal-to-noise ratio and is well compatible with immunostaining used in cell structural imaging. Complementarily, in single-molecule imaging mode, ITS activated by PIT are imaged with strong illumination light which also erases the activated ITS by photobleaching. The cycle of imaging and erasing enables the detection of integrin molecular tensions in real time and in live cells.

In cumulative imaging mode, PIT signal increases over a course of few minutes and formed in a ring-like pattern (Figure 1E, Video 1). The fluorescence intensity curve of PIT was obtained by averaging over 20 podosomes. Fluorescence signals from these podosomes have been synchronized by setting the time zero as the moment when detectable PIT signal starts to appear in individual podosomes. The slope of the curve indicates the PIT activity and shows that PIT is most active during the period of 4-10 min after detectable PIT started to manifest (240-630s in Figure 1F).

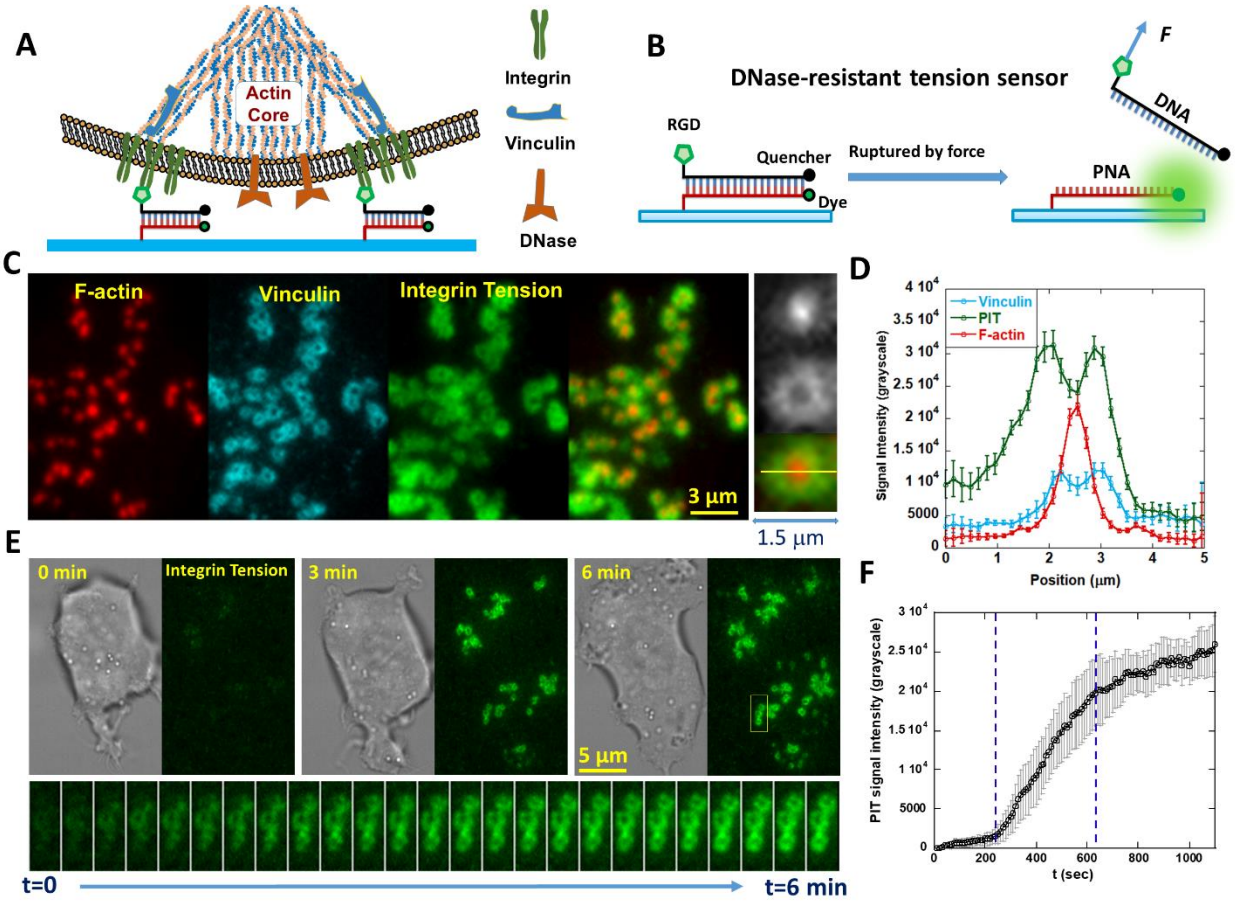

Figure 1. Imaging podosomal integrin tensions (PIT) with a DNase-resistant tension sensor. (**A**) Podosomes ubiquitously recruit DNase which degrades DNA-based tension sensors. (**B**) The construct of DNase-resistant PNA/DNA duplex-based integrative tension sensor (ITS), which becomes fluorescent after being ruptured by integrin tensions. (**C**) Co-imaging of F-actin, vinculin and PIT in THP-1 cells, incubated for 1 h prior to imaging. F-actin and vinculin were stained with phalloidin-Alexa 488 and anti-vinculin antibody, respectively. The inset shows that the actin core lies in the center of a PIT map. (**D**) Intensity profile of PIT, F-actin and vinculin in podosomes. Error bar represents standard deviations. N=20. (**E**)

Fluorescent PIT signal accumulated by time (Video 1). (**F**) Time-lapse fluorescence intensities of PIT signals averaged over 20 podosomes from multiple cells. Error bars represent standard deviations.

Imaging PIT at the single molecular tension level

ITS also enables single molecular tension imaging and super-resolution force imaging.[32] By imaging and erasing (by photobleaching) the activated tension sensors in each frame, we collect substantial number of photons from single activated tension sensors and erase them in 1-2 imaging frames, therefore recording molecular tension events with high sensitivity in live cells and in real time. Super-resolution force image can be obtained by localizing and assembling the molecular tension events in all imaging frames.

We have performed single integrin tension imaging in podosomes to gain more insight of the PIT (Figure 2A, Video 2). For the analysis of temporal nature of PIT generation, firstly, all frames were averaged into a single image (shown in green, Figure 2A), which shows the typical donut-shaped force patterns. This averaged force image helps to identify the podosome centers. The podosome centers are marked with magenta dots and we numbered 8 podosomes in the image. A super-resolution PIT image was obtained and displayed in Figure 2B. The spatial resolution of this force imaging technique has been calibrated to be around 50 nm.[32] At this length scale, however, PIT does not show apparent fine feature other than the donut-shaped pattern. PIT at the single molecule level was randomly and isotropically distributed around the center of adhesion ring over time (Figure S2).

The time-lapse force imaging provides an opportunity for us to study the spatiotemporal dynamics of single-molecule PIT in real time. We studied the potential correlation of PIT across the multiple podosomes in a cluster. It is known that podosomes may form in clusters, and previous study showed that podosomes in a cluster are connected by F-actin network.[11] Therefore, PIT of individual podosomes in one cluster are potentially correlated. As representative examples, we identified podosomes 1-2, 4-6 and 7-8 as three clusters and obtained time trace curves of PIT signals in these podosomes (Figure 2C). Consistent positive correlation was not identified for PIT signals of podosomes in cluster. Although podosomes 1 and 2 has 0.4 correlation value of forces, podosomes 4 and 5 has anti-correlation value -0.34. Podosomes 7 and 8 have a low anti-correlation value -0.04. We analyzed 30 paired podosomes (two neighboring podosomes) and 30 unpaired

podosomes (two podosomes with distance > 4 μm), and still did not observe strong correlation in either paired or unpaired podosomes (Figure 2D). These results suggest that podosome adhesive forces may be individually generated, despite being in cluster.

The temporal dynamics of real-time PIT appear periodic. Power spectrum (averaged over 8 podosomes) obtained by Fourier transformation of PIT temporal curves shows two local peaks of frequency at 0.053 Hz and 0.073 Hz, respectively, corresponding to 18.9 sec and 13.7 sec periods, reminiscent of a previous report that actin core protrusive force in podosomes has a periodic nature.[33]

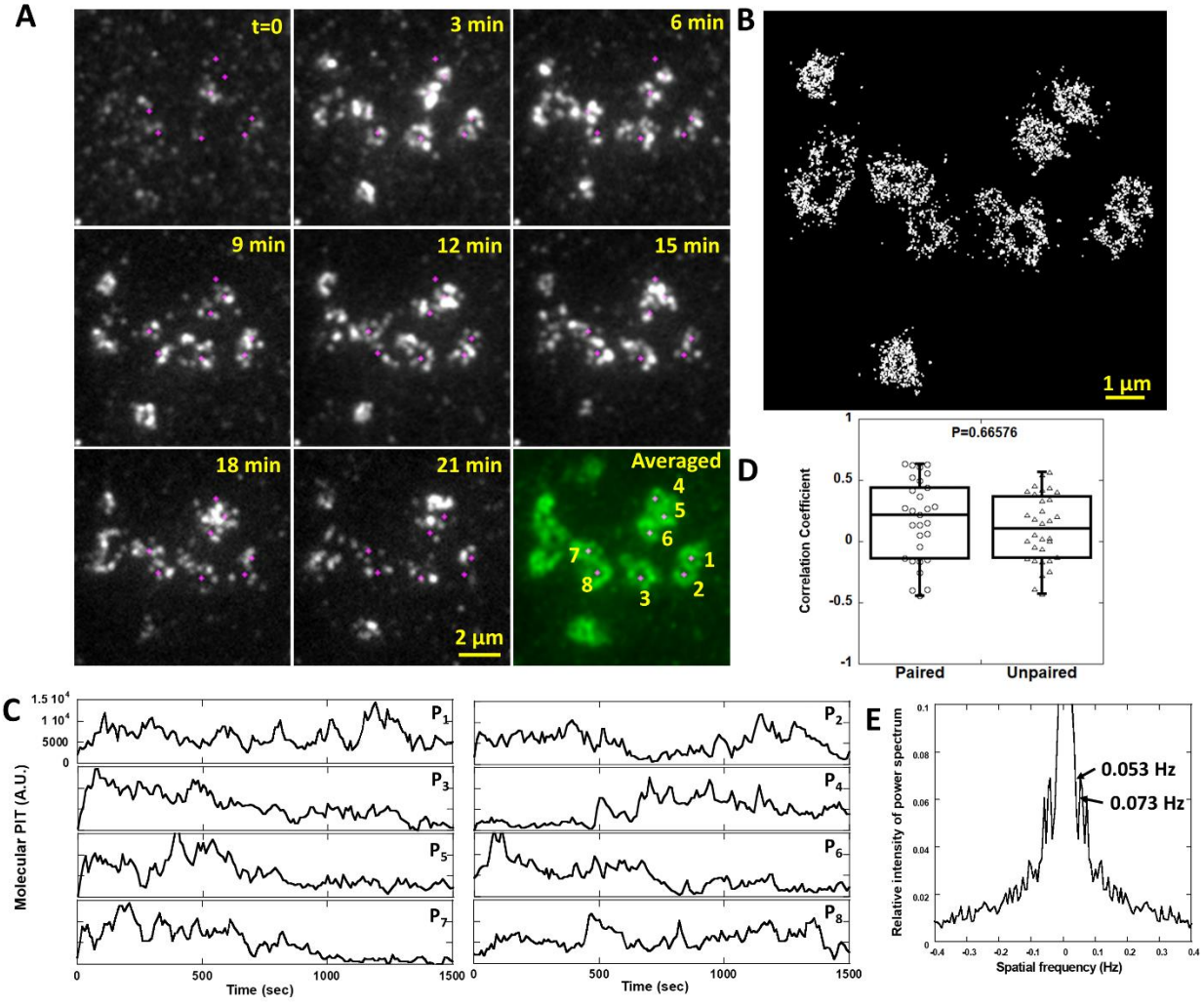

Figure 2. Imaging single-molecule integrin tensions in podosomes. (**A**) Time-lapse single integrin tension imaging in podosomes (Video 2, total time 25 min). The image in green is the average of all imaging frames to identify podosome centers (magenta dots). The THP-1 cells were incubated for 10-20 min prior

to video recording. (**B**) Super-resolution image of integrin tensions in podosomes assembled by molecular localization. (**C**) Time-lapse force signal intensity of individual podosomes 1-8. The fluorescence intensity of the PIT signal was calculated for each podosome in each frame. (**D**) The temporal correlation values of force signal intensities between paired podosomes (two neighboring podosomes) *versus* unpaired podosomes (two podosomes with a distance >4 μm). N=30, P value is evaluated by two-tailed tests. (**E**) Power spectrum of podosome force signals shows peak frequencies of 0.053 Hz and 0.073 Hz (periods of 18.9 sec and 13.7 sec).

Note that ITS is an irreversible tension sensor and will be locally consumed by integrin tensions. One should be mindful of ensuring that ITS local quantity is sufficient for examining PIT during the entire assay time. The surface density of ITS has been previously calibrated to be >2000/μm^2.[32] By comparing the fluorescence intensity of the PIT signal to that of a surface coated with quencher-null ITS, we determined that individual podosomes deplete 10-20% ITS locally during their lifetimes (data not shown). Therefore, ITS density is sufficiently high to examine the temporal dynamics of PIT.

Co-imaging of single integrin tensions and actin in podosomes

Previous studies have revealed that the actin cores of podosomes are capable of generating protrusive force on substrates, which has been calibrated and investigated by atomic force microscopy.[33, 34] This led to a biophysical model of podosomes in which the actin core protrudes into the ECM like a piston and the adhesion ring functions as a tensile anchor between podosomes and the substrates.[35] In light of these studies, we hypothesize that PIT in adhesion rings is correlated with core actin polymerization. We stained F-actin in live THP-1 cells with Phalloidin-Alexa555 by electroporation and imaged PIT and actin dynamics of podosomes simultaneously. By analyzing PIT (green) and F-actin (magenta) dynamics (Figure 3A, 3B and Video 3) along with several other cells under similar experimental conditions, we found that PIT dynamics are indeed positively correlated with actin dynamics (Figure 3C), suggesting that actin protrusion at the core region is likely related with PIT generation.

Next, we inhibited actin polymerization with latrunculin A and studied how it affects PIT generation. Because inhibiting actin polymerization throughout the whole incubation period is too drastic and results no podosome formation, we added actin inhibitor after podosomes have already

formed. Prior PIT signals were erased by photobleaching once the inhibitors were added and time-lapse imaging were conducted to monitor newly generated PIT signals in cumulative mode. This process of fluorescence recovery after photobleaching (force FRAP) is useful in examining the force generation ability in cells after a biochemical treatment. In the control group treated with DMSO (Dimethylsulfoxide, the solvent for the actin inhibitors), PIT signals soon recovered. However, PIT signal recovery was markedly reduced in the samples treated with 50 nM or 100 nM latrunculin A (Figure 3D-3E). Collectively, the correlation of PIT-actin dynamics and impeded PIT recovery with actin inhibition demonstrate that actin polymerization at the core region contributes to the generation of PIT.

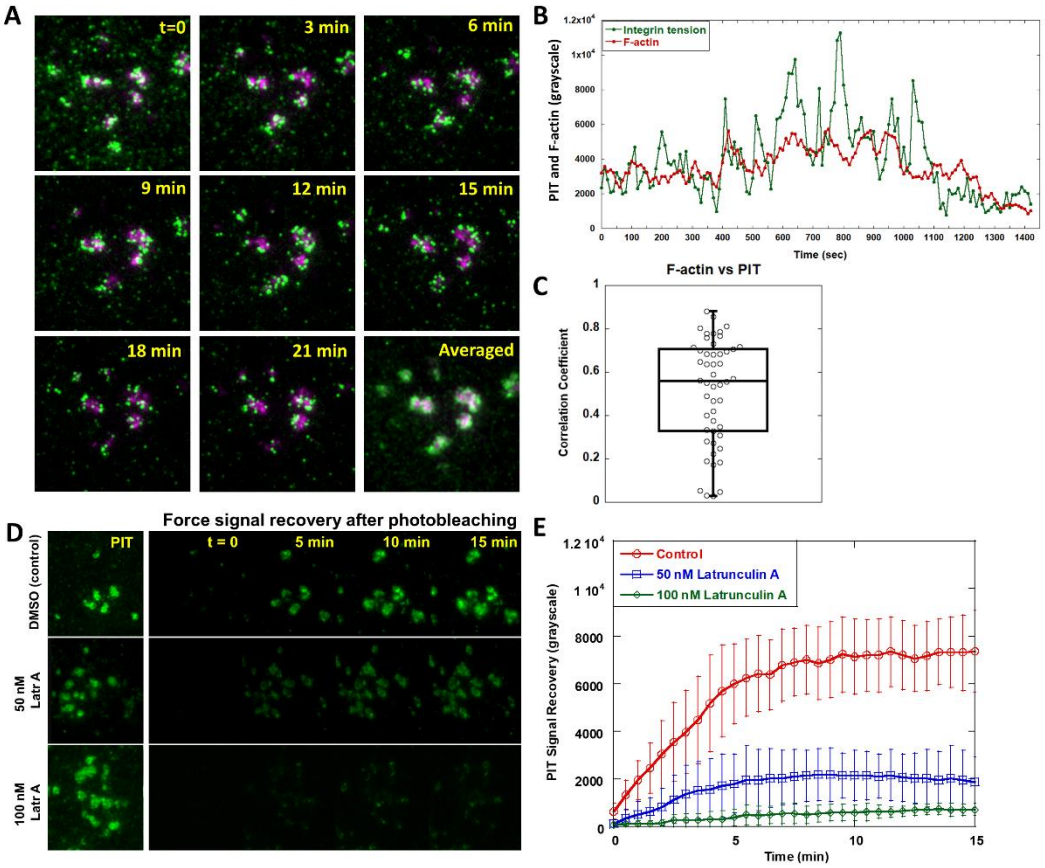

Figure 3. Temporal dynamics of single-molecule PIT and F-actin polymerization in podosomes. (**A**) Time-lapse imaging of single integrin tensions (green) and F-actin (magenta) in podosomes. (Video 3). Cells were incubated for 10-20 min prior to imaging. (**B**) Signal intensities of single integrin tensions and F-actin in a representative podosome. (**C**) Correlation coefficients between signal intensities of single PIT and F-actin

(N=50). (**D**) FRAP of PIT signals in podosomes after treatments of latrunculin A which was added after cells incubation on the surface for 30 min. (**E**) Time-series curves of PIT signal recovery.

Myosin II activated by ROCK, not MLCK, contributes to PIT generation

Next, we evaluated the contribution of myosin II activity to PIT by treating THP-1 cells with three types of myosin II inhibitors. First, 20 μM blebbistatin, a potent reagent disabling myosin II by inhibiting myosin ATPase,[36] was added to THP-1 cells. PIT signal was significantly reduced to 55% (Figs. 4A, 4B and 4E) while the actin cores and vinculin rings are not affected (Figs. 4F and 4G), suggesting that myosin II inhibition affects PIT generation but does not impact the structure formation of podosomes. Next, we inhibited ROCK (Rho-associated protein kinase) and MLCK (myosin light chain kinase) which are two upstream activators of myosin II, with the former one promoting myosin light chain (MLC) activity by inhibiting myosin phosphatase, and the latter one directly activating MLC. We treated the THP-1 cells with 20 μM Y-27632 which inhibits ROCK and 50 μM ML7 which inhibits MLCK, respectively. The results showed that Y-27632 significantly reduced the PIT signal by 50% (Figures 4C and 4E), while ML7 had no or marginal effect in reducing the PIT signal (Figures 4D and 4E). These results showed that ROCK, not MLCK, is critical for activating myosin II in the PIT generation.

These force imaging assays showed that myosin contractility significantly contributes to the PIT generation, but not to 100% extent. Even when myosin II is inhibited, the PIT was not completely abolished, suggesting there is other force source. Because we have shown that PIT signal positively correlates with F-actin dynamics and inhibition of F-actin polymerization reduces PIT recovery rate. The other force source should be actin core polymerization in podosomes. Collectively, we demonstrate that both myosin contractility and F-actin polymerization contribute to the generation of integrin tensions in podosomes.

Noticeably, in all these inhibition tests, even with drastic PIT reduction, F-actin signal in the core region and vinculin signal in the adhesion ring had little change, suggesting that podosome structural formation is insusceptible to myosin inhibition or PIT reduction. This intrigued us to further explore the force-structure interplay in podosomes and compare it to that in FAs, as podosomes and FAs share a similar set of structural and mechanotransducive proteins.

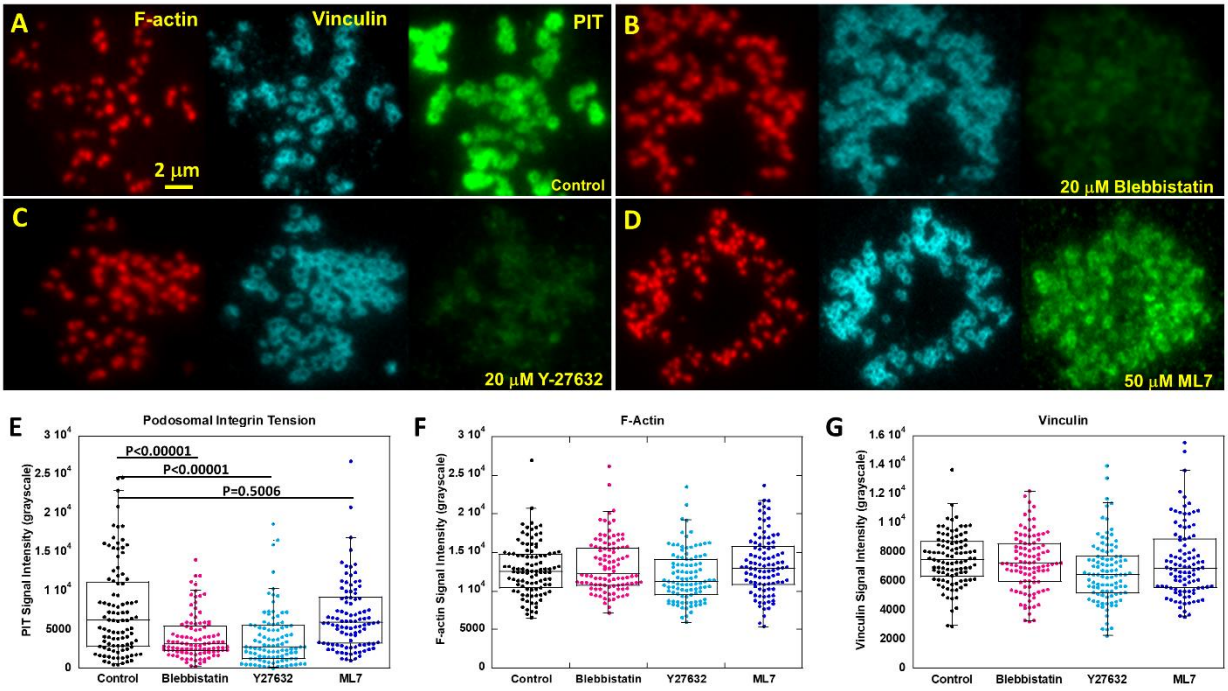

Figure 4. PIT under pharmaceutical intervention of myosin II. (A-D) F-actin, vinculin and PIT imaging in podosomes in the groups of control (DMSO), 20 μM blebbistatin, 20 μM Y-27632 and 50 μM ML7 treatments, respectively. (**E**) PIT signal intensities in the four groups of podosomes and integrin tensions in all four conditions. (**F**) F-actin signal intensities in the four groups of podosomes. (**G**) Vinculin signal intensities in the four groups of podosomes. Cells were incubated on imaging surfaces for 1 h prior to imaging. N=100 podosomes for each data point. All P values were evaluated by two-tailed tests.

Podosome formation is insusceptible to PIT reduction in contrast to FA formation.

Structure formation and force generation are interdependent in mechanotransducive units such as FAs. It has been well established that integrin-transmitted tensions are required for focal complexes maturing into FAs.[18, 37] Because podosomes bear similar protein components of FAs,[38, 39] and both of them are adhesive units transmitting force, it is tempting to assume that integrin-transmitted adhesive force in podosomes, the PIT, is also required for podosome formation. We conducted a comparative investigation between FA formation and podosome formation by manipulating integrin tensions in these two structures.

In Figure 5, both THP-1 (forming podosomes) and HeLa (forming FAs) were treated with DMSO as control (Figure 5A and 5C) and 20 μM blebbistatin (Figure 5B and 5D), respectively. All cells were plated on ITS surfaces to image integrin tensions, F-actin and vinculin simultaneously.

Inhibition of myosin II was confirmed to markedly reduce signal intensity of integrin tensions in podosomes (Figure 5E), but have no effect on the podosomal structure as the actin core and the vinculin ring are intact and podosome sizes are similar to those in the control group (Figure 5F). In contrast, both structure and signal intensity of integrin tensions in FAs changed drastically. Figure 5C shows normal stress fibers and FAs in HeLa cells and the typical streak force pattern caused by integrin tensions in FAs. Figure 5D shows that myosin II inhibition abolished stress fibers and significantly reduced FA sizes. Figure 5G and 5H showed that both signal intensity of integrin tensions and size of FAs in HeLa cells were significantly reduced by myosin inhibition. These results suggest that integrin tensions transmitted by integrin-ligand bonds, while being important for FA formation, are not critical for the formation of the podosome structures.

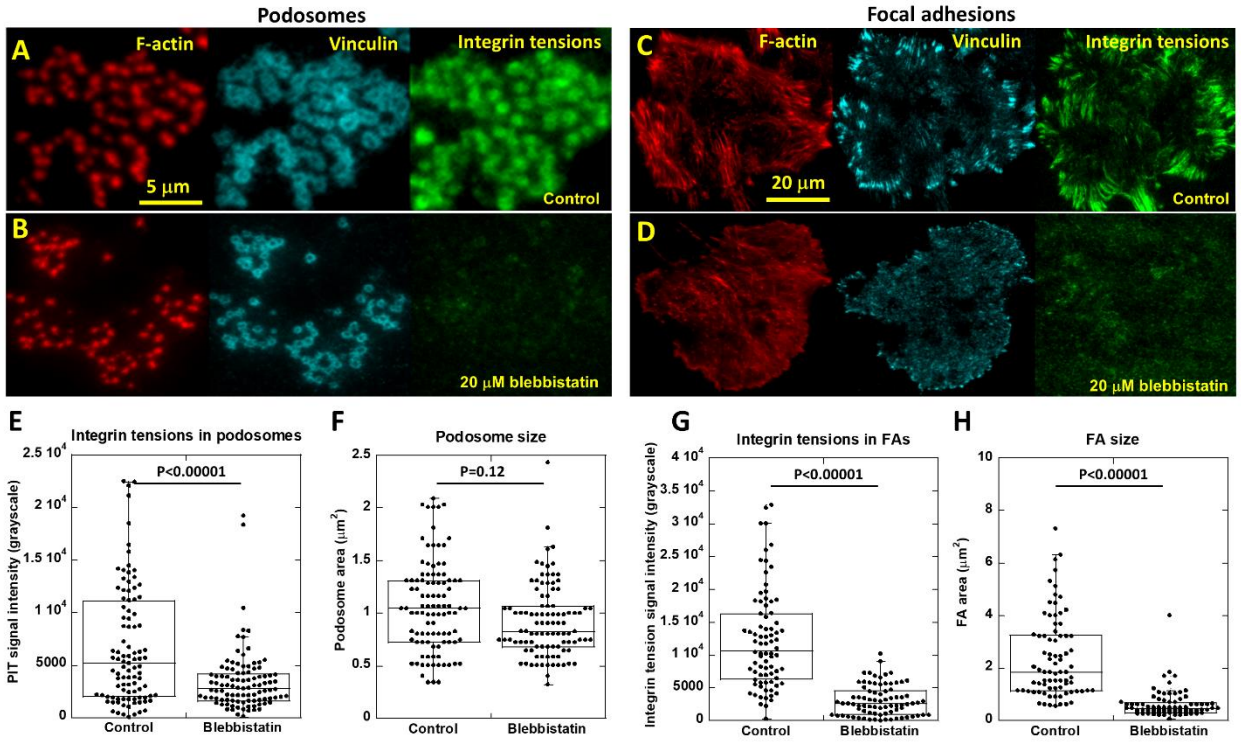

Figure 5. Structure formation and integrin tensions in podosomes and FAs with myosin II inhibition. (**A-B**) F-actin, vinculin and integrin tensions of THP-1 cells (forming podosomes) treated with DMSO (control) or 20 μM blebbistatin, respectively. (**C-D**) F-actin, vinculin and force images of HeLa cells (forming FAs) treated with DMSO or 20 μM blebbistatin, respectively. (**E**) Integrin tensions in podosomes in the two groups. (**F**) Podosome sizes in the two groups. (**G**) Integrin tensions in FAs in the two groups. (**H**) FA sizes in the two groups. Both types of cells were incubated on imaging surfaces for 1 h before fixation and

imaging. 100 podosomes and 80 FAs were analyzed for the corresponding data points. All P values were evaluated by two-tailed tests.

PIT signal intensity is uncorrelated with podosome structural signal intensity

THP-1 cells naturally exhibited strong heterogeneity in PIT generation, evident in Figure 4E and 5E. Podosomes bearing nearly zero detectable PIT were in fact not rare in our assays. However, the podosome structures have no clear relation to the PIT signal. Here, we conducted an experiment to monitor PIT, Vinculin and pFAK (phosphorylated focal adhesion kinase at tyrosine Y397) signals in podosomes without pharmaceutical intervention to cells. pFAK is known to be a signaling factor implicated in the formation of podosomes [40] and FAs, and have been shown to be mechanosensitive to external flow stress or integrin-matrix interaction.[41, 42] In Figure 6A and 6B, under the same culture condition, two THP-1 cells formed podosomes, with one cell generating strong PIT signal and the other producing low or undetectable PIT signal, demonstrating the intrinsic heterogeneity in PIT generation across cells. Despite the distinct levels of PIT signal intensities, no apparent difference in terms of F-actin, vinculin and pFAK signal intensities can be observed in podosomes of these two cells. To quantitatively evaluate the correlation between PIT signal and structural formation of podosomes. We calculated the PIT intensities of 120 podosomes from different cells, and categorized them into a “high-force” group and a “low-force” group with the median value of PIT signal intensities as the threshold. The signal intensities of F-actin, Vinculin and pFAK showed no significant different distribution between these two groups. (Figure 6C, 6D and 6E). The low correlation between PIT signal and structural signal in podosomes further suggests that integrin tensions at the cell-substrate interface is unrelated to podosome formation.

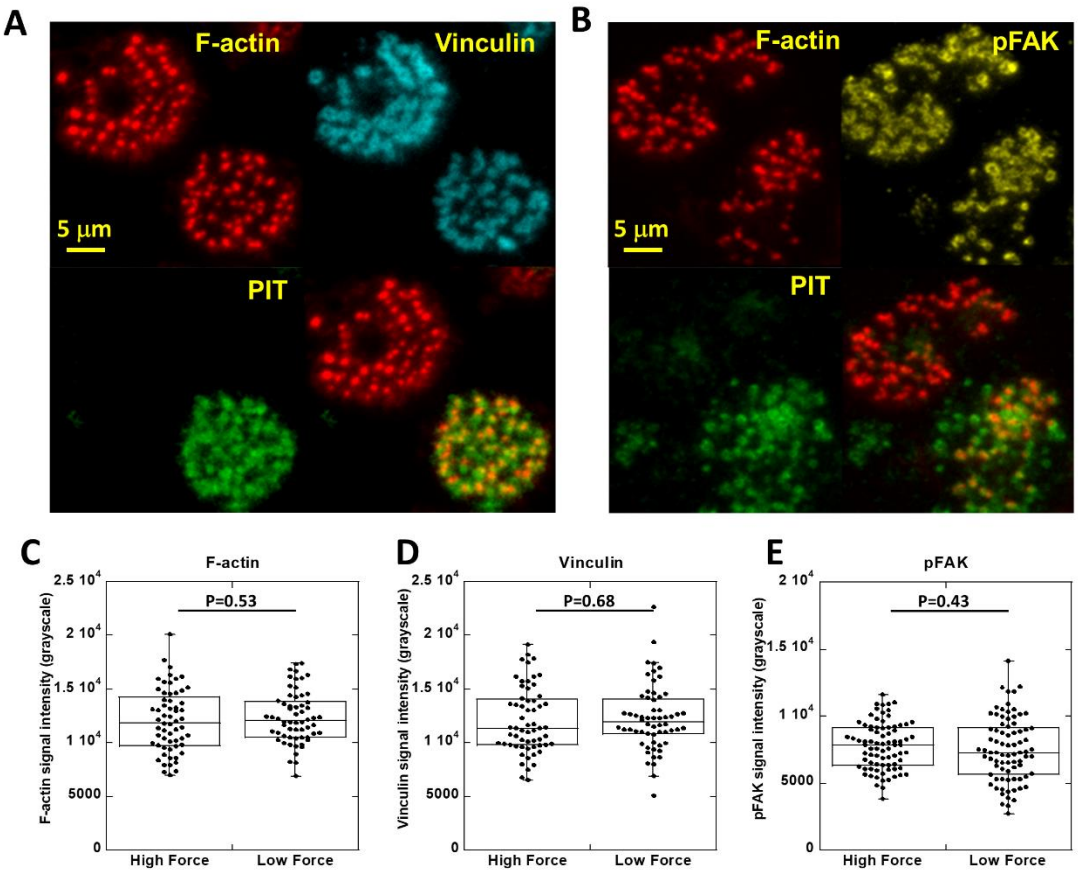

Figure 6. PIT is uncorrelated with vinculin and pFAK signal intensities in podosomes. (**A**) Two THP-1 cells with different PIT signals but similar vinculin signals. (**B**) Two THP-1 cells with different PIT signals but similar pFAK signals. (**D-F**) F-actin, Vinculin and pFAK signal intensities in two groups of podosomes separated in terms of the PIT signal intensity. The podosomes with PIT signals higher than the median value of all PITs is classified in the "high-force" group. Otherwise in the "low-force" group. Cells were incubated on imaging surfaces for 1 h before fixation and imaging. All P values were evaluated by two-tailed tests.

Integrin-ligand interaction is not required for podosome formation

By imaging integrin tensions in podosomes, we showed that podosome formation is insusceptible to PIT reduction and uncorrelated with PIT signal intensity, whereas FA formation is sensitive to integrin tension reduction. However, these data are still not sufficient to prove that PIT is not required for podosome formation, as myosin inhibition only reduces PIT activity in podosomes, not completely abolishing it. To further confirm that adhesive force transmitted by integrin-ligand bonds is truly dispensable for podosome formation, we prepared a ligand-free platform that supports cell adhesion by electrostatic adsorption while preventing integrin-substrate binding. We

coated glass surfaces with PLL-PEG (a poly-L-lysine backbone conjugated with multiple poly ethylene glycol branches) polymer. The PLL supports cell adhesion through electrostatic adsorption,[43] while the PEG branches repel organic materials such as proteins, thus forming a non-fouling coating on the surface.[44] PEG-functionalized surfaces have been commonly adopted for single molecule imaging that requires ultra-clean substrates.[45] The combination of PLL and PEG provides a useful strategy to support cell adhesion while suppressing mechanical interaction between membrane receptors and the substrate.

We plated both THP-1 and HeLa cells on fibronectin-coated surfaces and PLL-PEG functionalized surfaces, respectively, and imaged F-actin, Vinculin and pFAK. Imaging shows that podosomes in THP-1 cells exhibited normal formation on both surfaces (Figure 7A). The podosome size and pFAK signal intensity have no significant difference on the two surfaces (Figure 7B and 7C). In contrast, FAs and stress fibers in HeLa cells formed normally on the fibronectin-coated surface, but they were completely abolished on the PLL-PEG surface (Figure 7D and 7E), showing that the PLL-PEG surface functions as intended in preventing integrin-substrate interaction, and further testifies to that FA formation requires integrin-ligand interaction. There was low amount of pFAK in HeLa cells on the PLL-PEG surface, but its signal intensity is much lower than that on the fibronectin surface (Figure 7F). In addition, we have designed the integrin-blocking experiment to gain further evidence supporting that podosome formation does not requires extracellular integrin-ligand tensions. We plated HeLa and THP-1 cells on ITS surfaces without or with 100 μM soluble integrin RGD peptide ligand RGD. The result shows that the PIT intensity is markedly lower with soluble RGD treatment, suggesting that RGD blocks integrins in cell membrane (Figure S3). With integrins blocked by RGD, on PLL-PEG surfaces without immobilized integrin ligands, THP-1 cells still formed podosomes normally while FAs in HeLa cells were completely inhibited (Figure S4). Note that RGD does not block all integrin types. However, combined with PLL-PEG coating, RGD in solution further reduces the possibility of nonspecific integrin-substrate interaction. Therefore, this comparative study proves that extracellular integrin-ligand mechanical interaction and the associated adhesive force, while required for FA formation, are indeed dispensable for podosome formation.

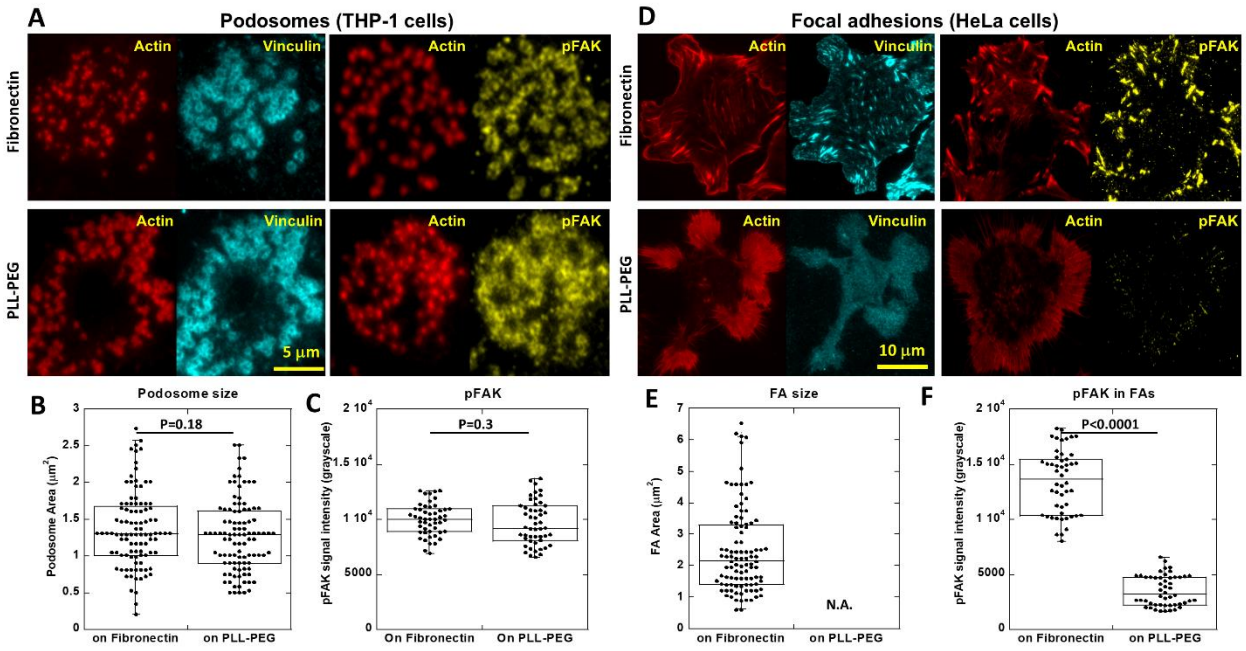

Figure 7. Podosomes and FA formation on fibronectin and PLL-PEG surfaces. (**A**) F-actin, vinculin and pFAK images of THP-1 cells on a fibronectin-coated surface and a PLL-PEG functionalized surface that supports cell adhesion but prevents integrin-substrate interaction. (**B**) Podosome sizes on the two surfaces. (**C**) pFAK signal intensities of podosomes on the two surfaces. (**D**) F-actin, vinculin and pFAK images of HeLa cells on a fibronectin-coated surface and a PLL-PEG functionalized surface. (**E**) FA sizes in HeLa cells on the two surfaces. (**F**) pFAK intensities in HeLa cells on the two surfaces. Both types of cells were incubated on surfaces for 1 h prior to imaging. All P values were evaluated by two-tailed tests.

To further reinforce the conclusion that podosome formation does not require integrin-ligand mechanical interaction, we developed another passivated substrate that blocks integrin-substrate interaction but supports THP-1 cell adhesion. It is well known that macrophages and neutrophils express abundant Fc receptors on the cell membrane which bind to antibodies including immunoglobin G (IgG).[46] We tested HeLa cells and THP-1 cells on rabbit IgG-coated glass surfaces. As shown in Figure S5, HeLa cells did not adhere on the IgG-coated surface at all, demonstrating that IgG coating does not support integrin-mediated adhesion. In contrast, THP-1 cells adhered and spread well on the IgG-coated surface, apparently through Fc receptor-mediated adhesion. Vinculin and F-actin imaging confirmed that THP-1 cells formed podosomes normally on the IgG-coated surface (Figure S5C and S5D), testifying to the conclusion that the integrin-ligand interaction is dispensable for podosome formation. We further demonstrated that podosomes can also form on integrin-ligand-free elastic substrates. A polydimethylsiloxane

(PDMS) gel surface was prepared and coated with PLL-PEG by physical adsorption. The PDMS gel elasticity was calibrated to be 12 kPa. We verified that this surface does not support FA formation in HeLa cells (data not shown). In contrast, THP-1 cells formed podosomes normally on the PDMS surface coated with PLL-PEG. As a positive control, the PDMS surface coated with fibronectin also support podosomes formation. Podosome formations are similar on both FN and PLL-PEG coated PDMS surface (Figure S6). This result confirmed that podosomes can form on elastic substrates without integrin ligands.

Conclusions

As adhesive and enzymatic units at the cell-matrix interface, podosomes are degradative to both matrix proteins and DNA,[12] making the DNA-based tension sensors problematic in podosome adhesive force imaging. Using a DNase-resistant tension sensor based on a PNA/DNA duplex, we imaged PIT in cumulative mode and in single-molecular tension mode, respectively. We found that PIT distribution exhibits a donut-shaped pattern, colocalized with the vinculin-rich adhesion rings as expected. Super-resolution force imaging enabled by molecular tension localization did not reveal finer spatial feature in PIT distribution other than the donut-shaped pattern. Real-time integrin tension imaging revealed that PIT exhibits signal intensity oscillation with 18.9 and 13.7 sec periods. The force oscillation may be related to the oscillatory behavior of podosome protrusive force against the substrate.[33, 47] We also show that integrin tension dynamics positively correlate with F-actin dynamics in the core region, and inhibiting actin polymerization reduced PIT signal intensity, suggesting that F-actin polymerization contributes to PIT generation. Inhibition of myosin II activity also resulted in the PIT reduction, suggesting that myosin II also contributes to PIT generation. In particular, myosin II activation by ROCK, not MLCK, is important for PIT generation. Collectively, both myosin II and F-actin polymerization contribute to the generation of PIT as podosome adhesive force. This is reminiscent of a previous study showing that these two sources contribute to podosomal protrusive force.[33] In contrast, another force study with the podosome-like structures in fibroblasts induced on fluidic lipid layer[23] suggested that myosin II does not participate in adhesive force generation in the podosome-like structure. This discrepancy might be caused by the different biomechanical nature between the podosome-like structures induced on fluidic surfaces and podosomes formed on solid surfaces.

We then studied the biomechanical role of integrin tensions in podosome formation and compared it to FA formation. As adhesive units at the cell-matrix interface, podosomes and FAs share a number of mechanotransducive proteins such as integrin, paxillin, talin, vinculin, pFAK, *etc.* Because it is well established that FA formation is governed by integrin-matrix interaction and dictated by integrin-ligand tensions,[48, 49] it is plausible that podosome formation may also depend on integrin-ligand tensions. However, our experiments collected multiple lines of evidence firmly proving that podosome formation does not require extracellular integrin-ligand tensions or even integrin-ligand interactions. First, we found that PIT signal reduction by myosin II inhibition had insignificant effect on the formation of actin cores and adhesion rings in podosomes. Second, there naturally exist THP-1 cells that form podosomes normally, but producing low or undetectable PIT signal, and PIT signal intensity is generally uncorrelated with the recruitment of F-actin, Vinculin and pFAK in podosomes. By examining hundreds of THP-1 cells, we found that about 30-35 % of cells showed no PIT but F-actin core and vinculin ring are present. Third, podosomes still formed normally on PLL-PEG-coated surfaces which abrogate integrin-ligand interaction but retain cell adhesion through electrostatic adsorption.[43] Furthermore, blocking the integrin with soluble integrin-ligand (cannot withstand tension) RGD on ITS and PLL-PEG surfaces shows insignificant effect on podosome formation. In contrast, FA formation were completely inhibited on such surfaces or under integrin-blocking condition. At last, podosomes also formed normally on IgG-coated surfaces which block integrin-substrate interaction but support THP-1 cell adhesion likely through Fc receptor-IgG interaction. All these lines of evidence prove that integrin-ligand tensions or integrin-substrate interactions are not required for podosome formation.

Prior to the direct PIT imaging in this work, it has been shown that myosin II contractility is not required for the integrity of podosome cores and rings,[11, 50] and podosome-like structures formed in fibroblasts on fluidic surfaces in the absence of traction force.[51] These results do not rule out the possibility that integrin-ligand tensions are needed to activate podosome formation, because neither method eliminated integrin-ligand tensions, as integrin-ligand tensions can be produced due to the actin core polymerization in place of myosin contractility, and fluidic lipid substrate do not negate integrin-ligand tensions in the vertical orientation. One previous literature also briefly mentioned podosome formation on PLL surface in dendritic cells (data not shown in the reference).[52] However, PLL without PEG polymer may allow non-specific integrin-substrate interaction. In this regard, by directly imaging integrin-ligand tensions and eliminating integrin-

ligand interactions through two types of passivated surfaces, our work provides direct and indisputable evidence showing that extracellular integrin-ligand tensions or interactions are truly dispensable in podosome formation. Therefore, integrin-ligand tensions play no role in podosome formation, and may only matter to podosome functions in cell migration and matrix remodeling, *etc.*

We speculated why podosomes can still form without integrin-ligand tensions or interactions. It is possible that intracellular domains of integrins in podosomes may still be linked to actin network, even without the extracellular domains attaching to the matrix. Due to the specific structure of podosomes, integrin-actin link may sustain tension without integrin-matrix interaction. As the adhesion ring (not adhering) is coupled with actin core with peripheral actin network,[53] integrin-actin tensile force can be generated due to actin core protruding against the cell membrane. The integrin-actin tensile force inside the cells could be sufficient to activate integrin signaling pathway and recruit adaptor proteins such as talin, vinculin, pFAK, *etc.*, eventually forming podosomes without the extracellular integrin-ligand interaction. In contrast, integrin-actin tensile force cannot be sustained in FAs without extracellular integrin-ligand bonds, as the integrin tensions in FAs are likely generated horizontally by stress fibers and requires integrins anchored on the substrates to avoid slippage. As a result, integrin-ligand bonds and associated force are required for integrin activation and structural formation in FAs. For the future study, direct imaging of integrin-actin tensile force within podosomes is expected to reveal more insights to the mechanobiology of podosome formation.

Methods

All nucleic acid-based sensors used in this study: The tension sensors or DNase sensors are based on dsDNA or PNA/DNA duplexes. They are synthesized by hybridizing the corresponding upper strand and lower strand (Table S1 in SI). All DNA strands with modifications were customized and purchased from Integrated DNA Technologies. All PNA strands were customized and purchased from PNA Bio. The DNA 1 (RGD-conjugated DNA) was synthesized by the protocol listed in next section.

Solutions of lower strand and upper strand were mixed at a molar ratio of 1:1.2 at a desired concentration, typically 10 μM, and annealed by heating the mixture to 90ºC and cooling it back to room temperature. These duplexes after hybridization can be stored in a freezer for more than a year without noticeable quality degradation.

Synthesis and purification of RGD-DNA: To synthesize RGD-DNA (DNA 1 in the table), a DNA product, /5ThioMC6-D/ GGG CGG CGA CCT CAG CAT/3BHQ_2/, was customized and purchased from Integrated DNA Technologies. /5ThioMC6-D/ represents a thiol modification that is latterly used for conjugating with an RGD peptide, a ligand binding to a variety of integrin types including integrin $\alpha_V\beta_3$, $\alpha_5\beta_1$, $\alpha_{IIb}\beta_3$, *etc.*

This DNA is conjugated with RGD and produces the DNA 1: /RGD/GGG CGG CGA CCT CAG CAT/3BHQ_2/. The conjugation is done as follows:

A solution of 500 mM TCEP (Tris (2-Carboxyethyl) phosphine) solution (77720, bond-breaker, ThermoFisher Scientific) and 500 mM EDTA in PBS (phosphate buffered saline) is prepared. This solution is to break the disulfide bond on DNA strand to a thiol group and makes it accessible for thiol-maleimide reaction. 10 μL of the above solution is added to 100 μL 2 mM thiol-DNA-BHQ2 in PBS. The solution is incubated for 30 min at room temperature (Solution 1).

In parallel, 10 mg RGD-NH_2 (PCI-3696-PI, Peptides International) is dissolved in 200 μL ultrapure water. The RGD-NH_2 solution is added to 2 mg solid sulfo-SMCC (A39268, Thermo Scientific) in a vial dipped in an ultra-sonicator to quickly dissolve the solid sulfo-SMCC. 22 μL 10× PBS is added to the solution afterwards, making the solution in final 1× PBS. It is advised to

avoid directly using 1× PBS to dissolve RGD-NH_2 and sulfo-SMCC, as sulfo-SMCC dissolves poorly in 1× PBS. This mixture is incubated for 10 min at room temperature (Solution 2).

Solution 1 and 2 are then mixed and incubated for 1 h at room temperature and overnight at 4 ºC. RGD is now conjugated to the DNA through sulfo-SMCC which is a heterolinker with a maleimide (reacting with the thiol of the DNA) at one end and an NHS ester (reacting with the amine of RGD-NH_2) at the other end. The purification of the product is performed in two steps. In the first step, the unreacted SMCC, RGD and TCEP are removed *via* ethanol precipitation (The protocol is common to find online). Next, DNA electrophoresis through 7.5% polyacrylamide gel is performed to further purify RGD-conjugated DNA (a lagging gel band) by removing unreacted DNA (a leading gel band). The RGD-DNA gel band is diced and soaked in PBS overnight at room temperature. RGD-DNA diffuses to PBS and is extracted by spinning the diced gel solution through a column with a filter (7326204, Bio-rad). The purification with electrophoresis can be skipped if the RGD-DNA purity checked by a low-scale DNA electrophoresis is more than 90%, which is often met by this synthesis protocol.

Imaging substrate preparation: The substrates for cell assays are glass-bottomed petridishes (D35-14-1.5-N, Cellvis) which support cell imaging with 100× oil lens. In our study, we immobilized ITS, poly-L-lysine-polyethylene glycol (PLL-PEG) or fibronectin (FN) on these glass surfaces.

ITS coating: To prepare this surface, we have adopted the biotin-neutravidin chemistry. Step 1: A solution of 200 µg/mL BSA-biotin (biotin-conjugated Bovine serum albumin, A8549, Sigma-Aldrich, USA) and 2 µg/mL FN (1918-FN, R&D System) in PBS buffer was added onto the well of a glass-bottom petri dish and incubated for 30 min at 4 ºC. BSA and FN both can physically adsorb on the glass surface, and FN was used to facilitate cell adhesion. The surface was washed with cold PBS three times. Step 2: The washed surface was incubated with a solution of 50 µg/mL neutravidin (31000, Thermo Fisher Scientific) in PBS for 30 min at 4ºC and washed with cold PBS three times. Step 3: The surface was incubated with the solution of 100 nM (for single molecule imaging this concentration was adjusted to 20 nM) PNA-based ITS (or other sensors) in PBS for 30 min at 4ºC and washed with PBS three times. Now the surface is ready for cell plating and further experiments.

FN coating: 5 μg/mL FN in PBS buffer was added onto the well of a glass-bottom petri dish and incubated for 30 min at 4 ºC. FN can physically adsorb on the glass surface, FN facilitate cell adhesion on the surface. The surface was washed with cold PBS for three times before cell plating.

PLL-PEG coating: PLL-PEG (poly-L-lysine conjugated with poly ethylene glycol) was customized and purchased from Nanosoft polymers. The PLL backbone has 100 repeats of poly-L-lysine. 20% of poly-L-lysine is conjugated with biotinylated PEG. Each PEG polymer has a molecular weight of 2 kDa (45 repeating units of ethylene glycol). A PLL-PEG coated glass surface was simply created by incubating 100 μg/mL PLL-PEG in pure water on the well of a glass-bottom petri dish for 30 min at room temperature. The surface was washed by pure water and became ready for use. PLL-PEG provides a cell adhesion surface by electrostatic adsorption while the PEG polymers repel proteins and suppress integrin-substrate interaction. ITS immobilization can be further immobilized on PLL-PEG surface by biotin-neutravidin interaction with a protocol similar to ITS coating with BSA-biotin, only the BSA-biotin is replaced with PLL-PEG.

Rabbit IgG coating: 100 μg/mL rabbit IgG (I5006-10MG, Sigma-Aldrich) in PBS buffer was added onto the well of a glass-bottom petri dish and incubated for 1 h at 4 ºC. IgG can physically adsorb on the glass surface. The surface was washed with cold PBS for three times before cell plating.

*PDMS gel casting***:** Polydimethylsiloxane (PDMS) gel was casted on the glass bottom petri-dish. The base and cross-linker (SYLGARD-184, Galco) with desired ratio (v/v base vs cross-linker, 50:1) were mixed and poured into the well of glass bottom petri dish. After 20 min, the mixture spontaneously spread on the glass surfaces and become flatten. The sample was then cured overnight at 70ºC on a hot plate. Stiffness of the PDMS gel samples was calibrated using Atomic Force Microscopy (Bioscope catalyst AFM, Bruker corporation) to be 12 kPa for the PDMS gel made with base and cross-linker at a 50:1 ratio. The procedure of PLL-PEG or fibronectin coatings on PDMS gel surfaces is the same as that on glass surfaces.

Cell culture and cell plating: Human monocytes THP-1 (TIB-202, ATCC) cells were cultured in RPMI-1640 medium (30-2001, ATCC) spiked with 2-mercaptoethanol (M3148, Sigma-Aldrich) to a final concentration of 0.05 mM and fetal bovine serum (30-2020, ATCC) to a final

concentration of 10 % (v/v). The macrophage activation was done with the treatment of 2 ng/mL transforming growth factor β-1 (240-B/CF, R&D System) for 24-36 hours. HeLa cells were cultured in DMEM medium (30-2002, ATCC) with 10 % (v/v) fetal bovine serum. For the experiments, cells (note that THP-1 is a suspension cell line but become adherent after TGF-β1 activation) were harvested as follows (unless mentioned otherwise): First, the culture medium was removed and washed with EDTA solution [recipe: 100 mL 10× HBSS +10 mL 1 M HEPES + 10 mL 7.5% sodium bicarbonate +2.4 mL 500 mM EDTA + 878 mL ultrapure water]. The cells were then incubated in EDTA solution (1 mL for 35 mm petri dish or 2 mL for the 25 cm^2 cell culture flask) inside an incubator with 5% CO_2 for 5 and 6 min for THP-1 and HeLa cells respectively. Cells were then pipetted off gently from the petri dish/culture flask and transferred into a centrifuge tube and centrifuged for 3 min at 350×g. Cell pellet was re-suspended with the culture medium and added onto the modified glass surface and incubated inside the incubator before static imaging, or directly on the petri dish mounted on the microscope for real-time imaging.

Note: For any experiment which is performed to compare between PLL-PEG *vs.* FN or ITS surfaces, serum-free medium was used. Serum contains various sticky proteins, which can adhere on surfaces and help cell adherence, so the surface may contain unwanted ligands other than our desired coating.

Cell electroporation with phalloidin: THP-1 cells are notoriously resistant to cell transfection, causing difficulty in expressing fluorescent proteins in live cells and imaging cell structure in real time. To investigate the temporal dynamics of actin nucleation and the force generation, dye-conjugated phalloidin was electroporated into THP-1 cells. A mixture of 15 µL electroporation buffer (45-0801, BTX), 5 µL [7.5 µM deoxy-ATP, 7.5 µM deoxy-GTP, and 5 µM deoxy-CTP in water] and 2 µL 3 U/mL AlexaFluor555-Phalloidin (173756, Abcam) was incubated for 15 min at room temperature prior to the electroporation. The Deoxy-ATP, deoxy-GTP and deoxy-CTP are known to prevent the aggregation of phalloidin.

Meanwhile, TGF-β1-activated THP-1 cells were detached from the cell culture flask and pelleted down by centrifugation (350×g for 3 min). The pellet was resuspended using the electroporation solution prepared in the previous step. This cell suspension was relocated to an electroporation cuvette (electrode gap 2 mm) which was electroporated with two consecutive square wave

electrical pulses at 100 V, 20 ms bandwidth and a 20-sec interval using an electroporation set up (ECM 830, BTX). Immediately after the electroporation, 1 mL of culture medium was added to the cuvette and cells were transferred onto the imaging platform. After 10 min, the medium containing electroporation buffer and free phalloidin-dye was removed and 2 mL of fresh medium was added and image acquisition was started immediately.

Immunostaining of Vinculin and pFAK: For the immunostaining, cells were fixed with 4% formaldehyde solution in PBS for 15 min at room temperature and subsequently permeabilized with 0.2 % Triton X-100 solution in PBS for 10 min at room temperature. The surface was then blocked with 5 mg/ mL BSA solution in PBS for 45 min at room temperature. For the staining of actin, Phalloidin-Alexa 405 (A30104, Thermo Fisher Scientific, USA) was used and the sample was incubated according to the supplier's instruction (typically 20-30 min at room temperature). The samples were washed with PBS for three times with 5 min incubation during each washing. The staining of vinculin and phosphor-Y397-FAK was performed in two steps. First, samples were treated with the solution of primary antibody anti-vinculin (90227, Millipore)/anti-phospho-Y397-FAK (700255, Thermo Fisher Scientific) in PBS for 1.5 h at room temperature and then washed with PBS for three times, with 5 min incubation during each washing. Fluorescent dye-labeled secondary antibody (ab175660, abcam, UK) solution in PBS was then added to the sample and incubated for 1h at room temperature and washed three time with PBS, with 5 min incubation during each washing.

Assays with pharmaceutical inhibitors: For static imaging, the inhibition experiment was performed as follows: EDTA treated cells were harvested by centrifugation in a centrifuge tube. The pellet was resuspended in complete medium with inhibitors at desired concentrations, namely, Latrunculin A (10010630, Cayman chemical) blebbistatin (Sigma Aldrich, B0560), Y-27632 (Y0503, Sigma-Aldrich) and ML-7 (I2764, Sigma-Aldrich), respectively. The cell suspension with corresponding inhibitor was plated on the imaging substrate and incubated in an incubator before imaging. For real-time force-FRAP (fluorescence recovery after photobleaching) imaging, cells were allowed to produce detectable force signal (during this time, no inhibitor was added to the medium) and then mounted on the microscope. After photobleaching all the historical force signal, medium with desired inhibitor was added and time-lapse imaging was performed.

Microscopy and data processing: All the static and real-time imaging was performed with a Nikon Ti-2E microscope using total internal reflection (TIRF) setup. For real-time imaging, lens heating method was adopted to provide warm environment to support cell viability. All imaging was acquired with an 100× oil immersion objective lens. Laser beams at 405, 488, 561 and 640 nm wavelengths were used as the excitation light sources. Image processing and analysis was done using the software (NIS-element) provided with the microscope combined with home-written MatLab code. Kaleidagraph software was used for graph plotting.

Single molecule imaging with a total reflection fluorescence microscope (TIRFM): Single molecule integrin force imaging was acquired with the same Nikon Ti-2E microscope. A 100× oil immersion objective lens was used for imaging and it was further magnified to 150× with a 1.5 X tube lens). First, the area of interest was made dark by photobleaching of activated sensors by laser (100% laser power) for 10 sec. In the following, the imaging was acquired at 60% laser intensity with 100 ms exposure time and 10 sec of frame interval. For single integrin-force event localization, STORM-analysis program was used (developed by X. Zhuang's group, https://storm-analysis.readthedocs.io/en/latest/). The output file with localized centers of molecular tension events was further analyzed with our MatLab code to obtain super-resolution force image.

AUTHOR INFORMATION

Corresponding Author

* **Xuefeng Wang**, Department of Physics and Astronomy, Iowa State University, Ames, IA 50011, USA; Email: xuefeng@iastate.edu

Authors:

Kaushik Pal, Department of Physics and Astronomy, Iowa State University, Ames, IA 50011, USA

Ying Tu, Department of Physics and Astronomy, Iowa State University, Ames, IA 50011, USA

Author Contributions

KP and XW designed the experiments, KP and YT performed the experiments, KP and XW analyzed the data and KP and XW co-wrote the manuscript.

Notes

The authors declare no competing financial interest.

ACKNOWLEDGMENT

This work was supported by National Institute of General Medical Sciences (1R35GM128747) and National Science Foundation (1825724).

Supporting Information

The Supporting Information is available free of charge online.

Control tests for PIT imaging with other DNA/DNA or DNA/PNA duplex constructs; Time-series images of single molecule PIT; Podosome formation with integrins blocked by soluble integrin ligands; Podosome formation on IgG-coated surfaces; Podosome formation on elastic substrates coated with PLL-PEG. A table with a list of all DNA or PNA strands used for the synthesis of sensors; Video captions for three videos.

REFERENCES

1. Buccione, R.; Orth, J. D.; McNiven, M. A., Foot and Mouth: Podosomes, Invadopodia and Circular Dorsal Ruffles. *Nat. Rev. Mol. Cell Biol.* **2004,** *5* (8), 647-657.
2. Linder, S.; Aepfelbacher, M., Podosomes: Adhesion Hot-Spots of Invasive Cells. *Trends Cell Biol.* **2003,** *13* (7), 376-385.
3. Linder, S., Invadosomes at a Glance. *J. Cell Sci.* **2009,** *122* (17), 3009-3013.
4. Murphy, D. A.; Courtneidge, S. A., The 'Ins' and 'Outs' of Podosomes and Invadopodia: Characteristics, Formation and Function. *Nat. Rev. Mol. Cell Biol.* **2011,** *12* (7), 413-426.
5. Akisaka, T.; Yoshida, H.; Suzuki, R.; Takama, K., Adhesion Structures and Their Cytoskeleton-Membrane Interactions at Podosomes of Osteoclasts in Culture. *Cell Tissue Res.* **2008,** *331* (3), 625-641.
6. Linder, S.; Cervero, P., The Podosome Cap: Past, Present, Perspective. *Eur. J. Cell Biol.* **2020,** *99* (5).
7. Gimona, M.; Buccione, R.; Courtneidge, S. A.; Linder, S., Assembly and Biological Role of Podosomes and Invadopodia. *Curr. Opin. Cell Biol.* **2008,** *20* (2), 235-241.
8. Georgess, D.; Machuca-Gayet, I.; Blangy, A.; Jurdic, P., Podosome Organization Drives Osteoclast-Mediated Bone Resorption. *Cell Adhes. Migr.* **2014,** *8* (3), 192-204.
9. Linder, S.; Nelson, D.; Weiss, M.; Aepfelbacher, M., Wiskott-Aldrich Syndrome Protein Regulates Podosomes in Primary Human Macrophages. *Proc. Natl. Acad. Sci. U. S. A.* **1999,** *96* (17), 9648-9653.
10. Baranov, M. V.; ter Beest, M.; Reinieren-Beeren, I.; Cambi, A.; Figdor, C. G.; van den Bogaart, G., Podosomes of Dendritic Cells Facilitate Antigen Sampling. *J. Cell Sci.* **2014,** *127* (5), 1052-1064.
11. van den Dries, K.; Meddens, M. B. M.; de Keijzer, S.; Shekhar, S.; Subramaniam, V.; Figdor, C. G.; Cambi, A., Interplay between Myosin Iia-Mediated Contractility and Actin Network Integrity Orchestrates Podosome Composition and Oscillations. *Nat. Commun.* **2013,** *4*.
12. Pal, K.; Zhao, Y.; Wang, Y.; Wang, X., Ubiquitous Membrane-Bound Dnase Activity in Podosomes and Invadopodia. *J. Cell Biol.* **2021,** *220* (7).
13. Gawden-Bone, C.; West, M. A.; Morrison, V. L.; Edgar, A. J.; McMillan, S. J.; Dill, B. D.; Trost, M.; Prescott, A.; Fagerholm, S. C.; Watts, C., A Crucial Role for Beta2 Integrins in Podosome Formation, Dynamics and Toll-Like-Receptor-Signaled Disassembly in Dendritic Cells. *J. Cell Sci.* **2014,** *127* (Pt 19), 4213-24.
14. Spanjaard, E.; de Rooij, J., Mechanotransduction: Vinculin Provides Stability When Tension Rises. *Curr. Biol.* **2013,** *23* (4), R159-R161.
15. Austen, K.; Ringer, P.; Mehlich, A.; Chrostek-Grashoff, A.; Kluger, C.; Klingner, C.; Sabass, B.; Zent, R.; Rief, M.; Grashoff, C., Extracellular Rigidity Sensing by Talin Isoform-Specific Mechanical Linkages. *Nat. Cell Biol.* **2015,** *17* (12), 1597-1606.
16. Turner, C. E., Paxillin and Focal Adhesion Signalling. *Nat. Cell Biol.* **2000,** *2* (12), E231-E236.
17. Parsons, J. T.; Horwitz, A. R.; Schwartz, M. A., Cell Adhesion: Integrating Cytoskeletal Dynamics and Cellular Tension. *Nat. Rev. Mol. Cell Bio.* **2010,** *11* (9), 633-643.
18. Wang, X. F.; Ha, T., Defining Single Molecular Forces Required to Activate Integrin and Notch Signaling. *Science* **2013,** *340* (6135), 991-994.
19. Zhang, Y.; Ge, C.; Zhu, C.; Salaita, K., DNA-Based Digital Tension Probes Reveal Integrin Forces During Early Cell Adhesion. *Nat. Commun.* **2014,** *5*, 5167.

20. Blakely, B. L.; Dumelin, C. E.; Trappmann, B.; McGregor, L. M.; Choi, C. K.; Anthony, P. C.; Duesterberg, V.; Baker, B. M.; Block, S. M.; Liu, D. R.; Chen, C. S., A DNA-Based Molecular Probe for Optically Reporting Cellular Traction Forces. *Nat. Methods* **2014,** *11* (12), 1229-1232.
21. Wang, Y. L.; LeVine, D. N.; Gannon, M.; Zhao, Y. C.; Sarkar, A.; Hoch, B.; Wang, X. F., Force-Activatable Biosensor Enables Single Platelet Force Mapping Directly by Fluorescence Imaging. *Biosens. Bioelectron.* **2018,** *100*, 192-200.
22. Zhao, B.; O'Brien, C.; Mudiyanselage, A. P. K. K. K.; Li, N. W.; Bagheri, Y.; Wu, R.; Sun, Y. B.; You, M. X., Visualizing Intercellular Tensile Forces by DNA-Based Membrane Molecular Probes. *J. Am. Chem. Soc.* **2017,** *139* (50), 18182-18185.
23. Glazier, R.; Brockman, J. M.; Bartle, E.; Mattheyses, A. L.; Destaing, O.; Salaita, K., DNA Mechanotechnology Reveals That Integrin Receptors Apply Pn Forces in Podosomes on Fluid Substrates. *Nat. Commun.* **2019,** *10*.
24. Wang, Y. L.; Zhao, Y. C.; Sarkar, A.; Wang, X. F., Optical Sensor Revealed Abnormal Nuclease Spatial Activity on Cancer Cell Membrane. *J. Biophotonics* **2019,** *12* (5).
25. Zhao, Y.; Sarkar, A.; Wang, X., Peptide Nucleic Acid Based Tension Sensor for Cellular Force Imaging with Strong Dnase Resistance. *Biosens. Bioelectron.* **2020,** *150*, 111959.
26. Ma, R.; Kellner, A. V.; Ma, V. P. Y.; Su, H. Q.; Deal, B. R.; Brockman, J. M.; Salaita, K., DNA Probes That Store Mechanical Information Reveal Transient Piconewton Forces Applied by T Cells. *Proc. Natl. Acad. Sci. U. S. A.* **2019,** *116* (34), 16949-16954.
27. Zhao, Y.; Wang, Y.; Sarkar, A.; Wang, X., Keratocytes Generate High Integrin Tension at the Trailing Edge to Mediate Rear De-Adhesion During Rapid Cell Migration. *iScience* **2018,** *9*, 502-512.
28. Xiong, J. P.; Stehle, T.; Zhang, R. G.; Joachimiak, A.; Frech, M.; Goodman, S. L.; Arnaout, M. A., Crystal Structure of the Extracellular Segment of Integrin Alpha V Beta 3 in Complex with an Arg-Gly-Asp Ligand. *Science* **2002,** *296* (5565), 151-155.
29. Rafiq, N. B. M.; Grenci, G.; Lim, C. K.; Kozlov, M. M.; Jones, G. E.; Viasnoff, V.; Bershadsky, A. D., Forces and Constraints Controlling Podosome Assembly and Disassembly. *Philos. Trans. R. Soc. B* **2019,** *374* (1779).
30. Destaing, O.; Saltel, F.; Geminard, J. C.; Jurdic, P.; Bard, F., Podosomes Display Actin Turnover and Dynamic Self-Organization in Osteoclasts Expressing Actin-Green Fluorescent Protein. *Mol. Biol. Cell* **2003,** *14* (2), 407-416.
31. Cox, S.; Rosten, E.; Monypenny, J.; Jovanovic-Talisman, T.; Burnette, D. T.; Lippincott-Schwartz, J.; Jones, G. E.; Heintzmann, R., Bayesian Localization Microscopy Reveals Nanoscale Podosome Dynamics. *Nat. Methods* **2012,** *9* (2), 195-200.
32. Zhao, Y. C.; Pal, K.; Tu, Y.; Wang, X. F., Cellular Force Nanoscopy with 50 Nm Resolution Based on Integrin Molecular Tension Imaging and Localization. *J. Am. Chem. Soc.* **2020,** *142* (15), 6930-6934.
33. Labernadie, A.; Bouissou, A.; Delobelle, P.; Balor, S.; Voituriez, R.; Proag, A.; Fourquaux, I.; Thibault, C.; Vieu, C.; Poincloux, R.; Charriere, G. M.; Maridonneau-Parini, I., Protrusion Force Microscopy Reveals Oscillatory Force Generation and Mechanosensing Activity of Human Macrophage Podosomes. *Nat. Commun.* **2014,** *5*, 5343.
34. Bouissou, A.; Proag, A.; Bourg, N.; Pingris, K.; Cabriel, C.; Balor, S.; Mangeat, T.; Thibault, C.; Vieu, C.; Dupuis, G.; Fort, E.; Leveque-Fort, S.; Maridonneau-Parini, I.; Poincloux, R., Podosome Force Generation Machinery: A Local Balance between Protrusion at the Core and Traction at the Ring. *Acs Nano* **2017,** *11* (4), 4028-4040.

35. Proag, A.; Bouissou, A.; Mangeat, T.; Voituriez, R.; Delobelle, P.; Thibault, C.; Vieu, C.; Maridonneau-Parini, I.; Poincloux, R., Working Together: Spatial Synchrony in the Force and Actin Dynamics of Podosome First Neighbors. *Acs Nano* **2015,** *9* (4), 3800-3813.
36. Kovacs, M.; Toth, J.; Hetenyi, C.; Malnasi-Csizmadia, A.; Sellers, J. R., Mechanism of Blebbistatin Inhibition of Myosin Ii. *J. Biol. Chem.* **2004,** *279* (34), 35557-63.
37. Balaban, N. Q.; Schwarz, U. S.; Riveline, D.; Goichberg, P.; Tzur, G.; Sabanay, I.; Mahalu, D.; Safran, S.; Bershadsky, A.; Addadi, L.; Geiger, B., Force and Focal Adhesion Assembly: A Close Relationship Studied Using Elastic Micropatterned Substrates. *Nat. Cell Biol.* **2001,** *3* (5), 466-472.
38. Block, M. R.; Badowski, C.; Millon-Fremillon, A.; Bouvard, D.; Bouin, A. P.; Faurobert, E.; Gerber-Scokaert, D.; Planus, E.; Albiges-Rizo, C., Podosome-Type Adhesions and Focal Adhesions, So Alike yet So Different. *Eur. J. Cell Biol.* **2008,** *87* (8-9), 491-506.
39. Albiges-Rizo, C.; Destaing, O.; Fourcade, B.; Planus, E.; Block, M. R., Actin Machinery and Mechanosensitivity in Invadopodia, Podosomes and Focal Adhesions. *J. Cell Sci.* **2009,** *122* (17), 3037-3049.
40. Yu, C. H.; Rafiq, N. B. M.; Krishnasamy, A.; Hartman, K. L.; Jones, G. E.; Bershadsky, A. D.; Sheetz, M. P., Integrin-Matrix Clusters Form Podosome-Like Adhesions in the Absence of Traction Forces. *Cell Rep.* **2013,** *5* (5), 1456-1468.
41. Zhou, D. W.; Fernandez-Yague, M. A.; Holland, E. N.; Garcia, A. F.; Castro, N. S.; O'Neill, E. B.; Eyckmans, J.; Chen, C. S.; Fu, J. P.; Schlaepfer, D. D.; Garcia, A. J., Force-Fak Signaling Coupling at Individual Focal Adhesions Coordinates Mechanosensing and Microtissue Repair. *Nat. Commun.* **2021,** *12* (1).
42. Li, S.; Butler, P.; Wang, Y. X.; Hu, Y. L.; Han, D. C.; Usami, S.; Guan, J. L.; Chien, S., The Role of the Dynamics of Focal Adhesion Kinase in the Mechanotaxis of Endothelial Cells. *P Natl Acad Sci USA* **2002,** *99* (6), 3546-3551.
43. Mazia, D.; Schatten, G.; Sale, W., Adhesion of Cells to Surfaces Coated with Polylysine - Applications to Electron-Microscopy. *J. Cell Biol.* **1975,** *66* (1), 198-200.
44. Fleminger, G.; Solomon, B.; Wolf, T.; Hadas, E., Effect of Polyethylene-Glycol on the Nonspecific Adsorption of Proteins to Eupergit-C and Agarose. *J. Chromatogr.* **1990,** *510*, 271-279.
45. Jain, A.; Liu, R. J.; Xiang, Y. K.; Ha, T., Single-Molecule Pull-Down for Studying Protein Interactions. *Nat. Protoc.* **2012,** *7* (3), 445-452.
46. Guilliams, M.; Bruhns, P.; Saeys, Y.; Hammad, H.; Lambrecht, B. N., The Function of Fcgamma Receptors in Dendritic Cells and Macrophages. *Nat. Rev. Immunol.* **2014,** *14* (2), 94-108.
47. Labernadie, A.; Thibault, C.; Vieu, C.; Maridonneau-Parini, I.; Charriere, G. M., Dynamics of Podosome Stiffness Revealed by Atomic Force Microscopy. *Proc. Natl. Acad. Sci. U. S. A.* **2010,** *107* (49), 21016-21021.
48. Pasapera, A. M.; Schneider, I. C.; Rericha, E.; Schlaepfer, D. D.; Waterman, C. M., Myosin Ii Activity Regulates Vinculin Recruitment to Focal Adhesions through Fak-Mediated Paxillin Phosphorylation. *J. Cell Biol.* **2010,** *188* (6), 877-890.
49. Choi, C. K.; Vicente-Manzanares, M.; Zareno, J.; Whitmore, L. A.; Mogilner, A.; Horwitz, A. R., Actin and Alpha-Actinin Orchestrate the Assembly and Maturation of Nascent Adhesions in a Myosin Ii Motor-Independent Manner. *Nat. Cell Biol.* **2008,** *10* (9), 1039-U36.
50. van den Dries, K.; Schwartz, S. L.; Byars, J.; Meddens, M. B. M.; Bolomini-Vittori, M.; Lidke, D. S.; Figdor, C. G.; Lidke, K. A.; Cambi, A., Dual-Color Superresolution

Microscopy Reveals Nanoscale Organization of Mechanosensory Podosomes. *Mol. Biol. Cell* **2013,** *24* (13), 2112-2123.
51. Yu, C. H.; Rafiq, N. B. M.; Krishnasamy, A.; Hartman, K. L.; Jones, G. E.; Bershadsky, A. D.; Sheetz, M. P., Integrin-Matrix Clusters Form Podosome-Like Adhesions in the Absence of Traction Forces. *Cell Rep.* **2013,** *5* (5), 1456-1468.
52. van den Dries, K.; van Helden, S. F. G.; te Riet, J.; Diez-Ahedo, R.; Manzo, C.; Oud, M. M.; van Leeuwen, F. N.; Brock, R.; Garcia-Parajo, M. F.; Cambi, A.; Figdor, C. G., Geometry Sensing by Dendritic Cells Dictates Spatial Organization and Pge(2)-Induced Dissolution of Podosomes. *Cell Mol. Life Sci.* **2012,** *69* (11), 1889-1901.
53. van den Dries, K.; Nahidiazar, L.; Slotman, J. A.; Meddens, M. B. M.; Pandzic, E.; Joosten, B.; Ansems, M.; Schouwstra, J.; Meijer, A.; Steen, R.; Wijers, M.; Fransen, J.; Houtsmuller, A. B.; Wiseman, P. W.; Jalink, K.; Cambi, A., Modular Actin Nano-Architecture Enables Podosome Protrusion and Mechanosensing. *Nat. Commun.* **2019,** *10*.